

13. Unlike peripheral blood mononuclear cells or adherence-purified monocytes (6), the production of p70 (as opposed to p40) by elutriated human monocytes is dependent on preincubation with IFN- $\gamma$  (C. L. Karp, unpublished data).
14. MV strains tested in addition to wild-type Edmonston included a Finnish wild-type isolate (courtesy of A. Salmi) [R. Vainionpaa, B. Ziola, A. A. Salmi, *Acta Pathol. Microbiol. Immunol. Scand. B* **86**, 379 (1978)], as well as JM and Chicago-1 (courtesy of P. Rota).
15. MV preparations (and uninfected Vero cell lysates) were inactivated by short-wave UV irradiation for 55 min in the cold. After irradiation, stocks were kept at 4°C for at least 3 hours and were subsequently frozen before use. Such stocks were used to treat monocytes (17) at a (preirradiation) MOI of 5.
16. TNF- $\alpha$  and IL-6 were measured by ELISA (Pharmingen); ELISA measurement of MIP-1 $\alpha$  and MIP-1 $\beta$  was done as previously described [H. Schmidt-Mayrova *et al.*, *Proc. Natl. Acad. Sci. U.S.A.* **93**, 700 (1996)].
17. D. G. Mayernik, A. Haq, J. J. Rinehart, *J. Leukocyte Biol.* **56**, 551 (1984).
18. G. Zurawski and J. E. de Vries, *Immunol. Today* **15**, 19 (1994); S. K. Durum and J. J. Oppenheim, in *Fundamental Immunology*, W. E. Paul, Ed. (Raven, New York, ed. 3, 1993), pp. 801–833.
19. IL-10 was measured by ELISA (Pharmingen).
20. MV- or mock-infected monocytes were stimulated with IFN- $\gamma$ -LPS or IFN- $\gamma$ -SAC in the presence of a neutralizing mAb to IL-10 or of an isotype control (both from Pharmingen).
21. Neutralizing rabbit polyclonal (R & D Systems) and monoclonal (Genzyme) antibodies to TGF- $\beta$  were used with appropriate isotype control antibodies from the same manufacturers.
22. PGE2 measurement was by RIA as previously described [L. M. Wahl, in *Manual of Macrophage Methodology*, H. B. Herscovitz, H. T. Holden, J. A. Bellanti, A. Ghaffar, Eds. (Dekker, New York, 1981), pp. 423–429].
23. IL-4 measurement was by means of an ELISA with a sensitivity of 10 to 20 pg/ml (Pharmingen). IL-13 was measured by RT-PCR at 40 cycles [C. L. Karp *et al.*, *J. Clin. Invest.* **91**, 1644 (1993)].
24. D. Nanche *et al.*, *J. Virol.* **67**, 6025 (1993); R. E. Dorig, A. Marciel, A. Chopra, C. D. Richardson, *Cell* **75**, 295 (1993).
25. M. K. Liszewski, T. W. Post, J. P. Atkinson, *Annu. Rev. Immunol.* **9**, 431 (1991).
26. D. Gerlier *et al.*, *J. Gen. Virol.* **75**, 2163 (1994); O. Nussbaum *et al.*, *J. Virol.* **69**, 3341 (1995); M. Manchester *et al.*, *Proc. Natl. Acad. Sci. U.S.A.* **92**, 2303 (1995); E. M. Adams, M. C. Brown, M. Nunge, M. Krych, J. P. Atkinson, *J. Immunol.* **147**, 3005 (1991).
27. M. Manchester *et al.*, *Proc. Natl. Acad. Sci. U.S.A.* **92**, 2303 (1995); R. E. Dorig, A. Marciel, A. Chopra, C. D. Richardson, *Cell* **75**, 295 (1993); S. W. Cho, T. J. Oglesby, B. L. Hsi, E. M. Adams, J. P. Atkinson, *Clin. Exp. Immunol.* **83**, 257 (1991).
28. Monocytes were stimulated with IFN- $\gamma$ -SAC or IFN- $\gamma$ -LPS after preincubation with ascites-derived antibodies GB24 or TRA-2-10 (both courtesy of J. Atkinson) or isotype control mAb to V3 (courtesy of J. Hildreth), all at a final dilution of 1:333. Monocytes were similarly stimulated after preincubation with purified J4-48 antibody (2.6  $\mu$ g/ml) (Immunotech) or isotype control antibody to trinitrophenol (Pharmingen). All antibodies to CD46 were murine immunoglobulin G<sub>1</sub>.
29. K. R. Kalli *et al.*, *J. Exp. Med.* **174**, 1451 (1991).
30. D. T. Fearon and R. H. Carter, *Annu. Rev. Immunol.* **13**, 127 (1995).
31. S. J. James, *Microbiol. Rev.* **59**, 533 (1995).
32. M. S. Hirsch and J. Curran, in *Virology*, B. N. Fields *et al.*, Eds. (Lippincott-Raven, Philadelphia, PA, ed. 3, 1996), pp. 1953–1973.
33. J. Chehimi *et al.*, *J. Exp. Med.* **179**, 1361 (1994).
34. C. F. Ebenbichler *et al.*, *ibid* **174**, 1417 (1991); N. M. Thielens, I. M. Bally, C. F. Ebenbichler, M. P. Dierich, G. J. Arlaud, *J. Immunol.* **151**, 6583 (1993); N. Thieblemont, N. Haeflner-Cavaillon, L. Weiss, F. Maillet, M. D. Kazatchkine, *AIDS Res. Hum. Retrovir.* **9**, 229 (1993); H. Stoiber, R. Schneider, J. Janatova, M. P.

Dierich, *Immunobiology* **193**, 98 (1995). B. M. Solder, *Immunol. Lett.* **22**, 135 (1989); G. T. Spear, A. L. Landay, B. L. Sullivan, B. Dittell, T. F. Lint, *J. Immunol.* **144**, 1490 (1990); P. Marschang *et al.*, *AIDS* **7**, 903 (1993); M. P. Dierich *et al.*, *Immunol. Today* **14**, 435 (1993).

35. We thank J. Atkinson and J. Hildreth for mAbs and M. Wills-Karp, D. R. Moller, and A. Valsamakis for

useful discussions. Supported in part by NIH grants AI01223 (C.L.K.); AI35149 and AI23047 (D.E.G.); and AI34412, CA20833, CA10815, and CA32898 (G.T., M.W.); the Peggy Meyerhoff Pearlstone Foundation (J.M.A.); and World Health Organization grant V21/181/67 (D.E.G.).

12 March 1996; accepted 13 May 1996

## Structure of the Amino-Terminal Core Domain of the HIV-1 Capsid Protein

Rossitza K. Gitti,\* Brian M. Lee,\* Jill Walker, Michael F. Summers,† Sanghee Yoo, Wesley I. Sundquist†

The three-dimensional structure of the amino-terminal core domain (residues 1 through 151) of the human immunodeficiency virus-type 1 (HIV-1) capsid protein has been solved by multidimensional heteronuclear magnetic resonance spectroscopy. The structure is unlike those of previously characterized viral coat proteins and is composed of seven  $\alpha$  helices, two  $\beta$  hairpins, and an exposed partially ordered loop. The domain is shaped like an arrowhead, with the  $\beta$  hairpins and loop exposed at the trailing edge and the carboxyl-terminal helix projecting from the tip. The proline residue Pro<sup>1</sup> forms a salt bridge with a conserved, buried aspartate residue (Asp<sup>51</sup>), which suggests that the amino terminus of the protein rearranges upon proteolytic maturation. The binding site for cyclophilin A, a cellular rotamase that is packaged into the HIV-1 virion, is located on the exposed loop and encompasses the essential proline residue Pro<sup>90</sup>. In the free monomeric domain, Pro<sup>90</sup> adopts kinetically trapped *cis* and *trans* conformations, raising the possibility that cyclophilin A catalyzes interconversion of the *cis*- and *trans*-Pro<sup>90</sup> loop structures.

The most distinctive architectural feature of HIV-1 and other lentiviruses is an electron-dense conical capsid core that surrounds the RNA genome at the center of the virus (1). The core structure is not present in freshly budded, immature virions because the membrane-bound Gag polyprotein dictates the initial steps in viral assembly and budding. Concomitant with budding, however, Gag is proteolytically processed by the viral protease to produce three new structural proteins: p17 matrix (MA), p24 capsid (CA), and p7 nucleocapsid (NC) (2). The processed proteins subsequently undergo a dramatic structural rearrangement, termed “maturation,” in which the capsid protein condenses to form the conical core structure surrounding the NC-RNA copolymer, while the matrix protein remains bound to the viral membrane.

In addition to forming the core of the mature virion, extensive genetic analyses have revealed that HIV-1 CA performs essential roles during viral assembly and disassembly (3–5). Mutations and deletions within the final 80 amino acids of the 231-amino acid capsid sequence can impair or abolish viral

assembly, which suggests that the COOH-terminus of CA encompasses a Gag oligomerization domain. In contrast, mutations in the NH<sub>2</sub>-terminal two-thirds of CA often give rise to viruses that can assemble and bud but are nevertheless noninfectious. Many of these mutant viruses exhibit aberrant capsid morphologies. These observations indicate that sequences in the NH<sub>2</sub>-terminal two-thirds of CA are essential for establishing the conical capsid core morphology and probably also play a role in viral penetration or uncoating, or both.

Another essential function of HIV-1 CA is to bind to the human cellular proline rotamase cyclophilin A (CypA). This direct interaction results in the packaging of ~200 copies of CypA into each HIV-1 virion (6–8). CypA packaging can be blocked by treatment of cultured virus with the immunosuppressive drug cyclosporine or its analogs (6–9), which bind tightly in the active site of CypA (10). CypA packaging can also be blocked by mutations throughout the NH<sub>2</sub>-terminal two-thirds of CA (6–8). Although the precise function of CypA is not yet clear, virions lacking the enzyme appear normal by standard biochemical assays but are poorly infectious. Cyclophilin A therefore performs an essential role early in the viral life cycle (8, 11), possibly accelerating the isomerization of a key capsid proline residue and facilitating viral uncoating.

High-resolution structural information

R. K. Gitti, B. M. Lee, J. Walker, M. F. Summers, Howard Hughes Medical Institute and Department of Chemistry and Biochemistry, University of Maryland Baltimore County, Baltimore, MD 21228, USA. S. Yoo and W. I. Sundquist, Department of Biochemistry, University of Utah, Salt Lake City, UT 84132, USA.

\*These authors contributed equally to the structure determination.

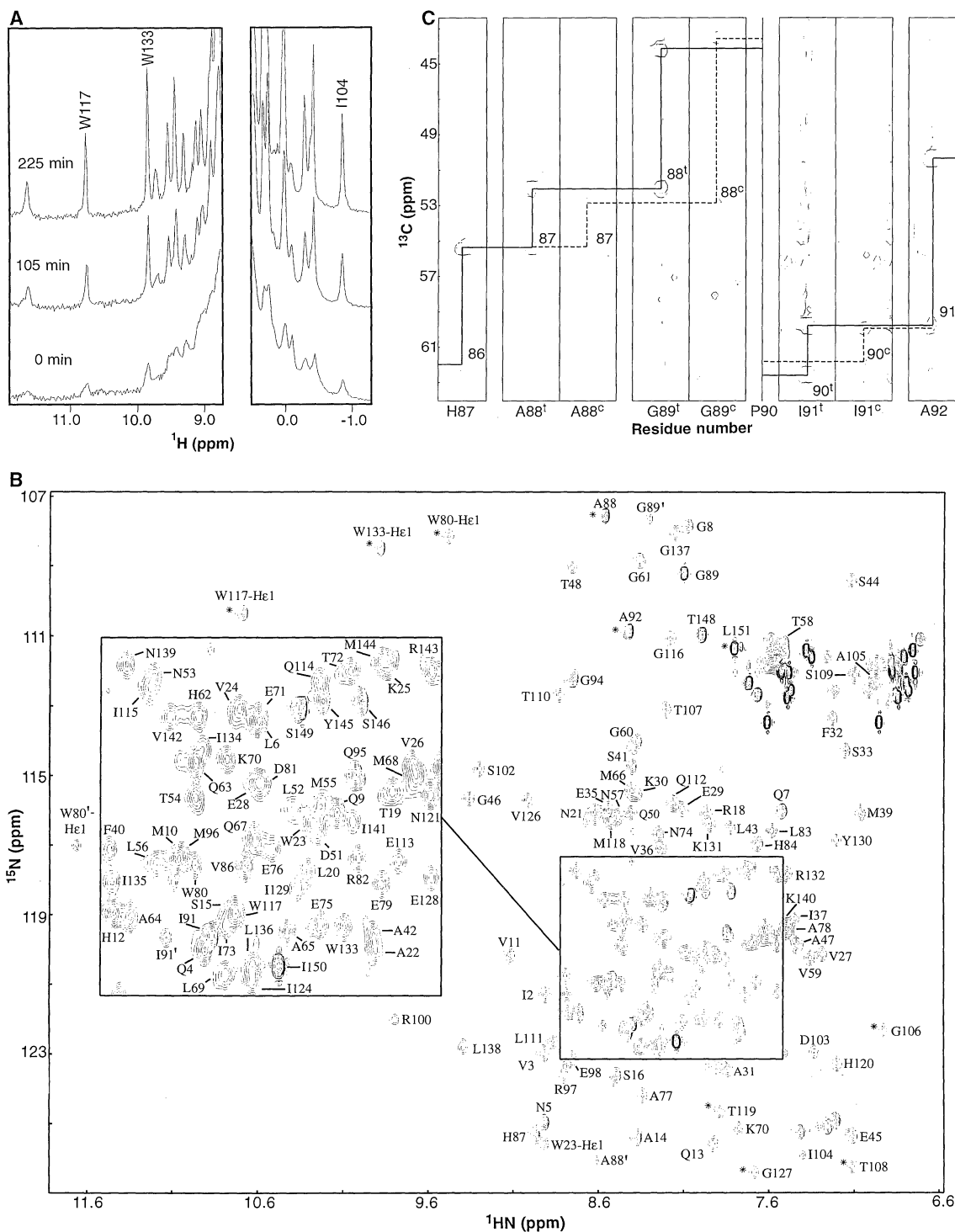
†To whom correspondence should be addressed.

has not been available for any retroviral capsid protein. Structural studies of HIV-1 CA are complicated by the fact that the native protein can form a complex mixture of oligomers in solution, including dimers, tetramers, dodecamers, spheres, fibers, and tubes (12). Although HIV-1 CA has been successfully cocrystallized with an antibody

fragment (13), the crystal structure has yet to be reported. In an attempt to define domains that are amenable to nuclear magnetic resonance (NMR) structural studies, we subjected native and mutant recombinant capsid proteins to limited proteolysis and monitored them by NMR spectroscopy and SDS-polyacrylamide gel electrophore-

sis (SDS-PAGE) (14). These experiments revealed that the NH<sub>2</sub>-terminal (core) domain of the protein was resistant to limited proteolysis, whereas the COOH-terminal (assembly) domain, which contains a highly conserved 20-residue sequence termed the major homology region (MHR), was susceptible to digestion. Proteolytic cleavage of

**Fig. 1.** (A) Resolved downfield (left) and up-field (right) portions of 1D <sup>1</sup>H NMR spectra obtained at indicated times during limited trypsin digestion of CA<sub>E159D</sub> (14). Resolved signals do not shift but narrow considerably upon proteolysis (by as much as fourfold), reflecting a decrease in molecular weight from 51 kD for the dimer to ~17 kD for the cleaved, monomeric core domain. The 1D NMR spectrum of native CA is also very similar to that of CA<sub>E159D</sub>, but the native protein is more resistant to proteolysis (33). (B) 2D <sup>1</sup>H-<sup>15</sup>N HSQC spectrum (18) obtained for recombinant HIV-1 CA<sub>151</sub>, including an expansion of the most crowded region (boxed) (15). Assignments are included for all backbone and Trp side chain NH pairs [unlabeled signals correspond to side chain NH<sub>2</sub> (Asn and Gln) and NH (Arg) groups]. Signals resulting from the *cis*-Pro<sup>90</sup> minor conformer and a minor conformer involving the flipped side chain of Trp<sup>80</sup> are labeled with primes, and signals that are folded in the <sup>15</sup>N dimension are denoted by an asterisk. (C) Selected <sup>13</sup>C, <sup>1</sup>H strips from the 3D HNCA data (18) showing the two sets of resonances observed for residues in close proximity to Pro<sup>90</sup>. The solid lines denote interresidue connectivities for the major (*trans*-Pro<sup>90</sup>) conformer, and the dotted lines connect signals of the minor (*cis*-Pro<sup>90</sup>) conformer. Residue assignments are given at the bottom of the figure, and interresidue correlations to preceding Cα carbons are labeled within the figure (c and t refer to signals associated with the *cis*-Pro<sup>90</sup> and *trans*-Pro<sup>90</sup> conformers, respectively).



the assembly domain was particularly efficient for a CA mutant containing a Glu<sup>159</sup> → Asp<sup>159</sup> (E159D) (15) substitution in the MHR (CA<sub>E159D</sub>) (14, 16). As shown in Fig. 1A, resolved <sup>1</sup>H NMR signals observed for CA<sub>E159D</sub> narrow considerably upon proteolysis but do not undergo frequency shifts, which indicates that the intact capsid protein is, in fact, composed of two distinct domains and that limited proteolysis does not alter the structure of the NH<sub>2</sub>-terminal core domain.

In order to produce a homogeneous protein for structural studies, the HIV-1 capsid core domain (residues 1 through 151; CA<sub>151</sub>) was expressed in *Escherichia coli* and purified to homogeneity (17). The <sup>1</sup>H NMR spectrum of CA<sub>151</sub> was again similar to that of the partially digested protein sample, indicating that the expressed and proteolyzed domains adopt the same structure in solution. Gradient-enhanced triple-resonance NMR methods, including four-dimensional (4D) <sup>15</sup>N-<sup>13</sup>C- and <sup>13</sup>C-<sup>13</sup>C-edited nuclear Overhauser effect spectroscopy (NOESY) experiments, were applied to <sup>15</sup>N and <sup>15</sup>N-<sup>13</sup>C isotopically labeled CA<sub>151</sub> proteins, allowing assignment of the backbone and side chain signals (18). The quality and resolution of the data are reflected in the 2D <sup>1</sup>H-<sup>15</sup>N heteronuclear single-quantum coherence (HSQC) spectrum shown in Fig. 1B. Two sets of signals (relative ratio, 86:14) were observed for residues within the CypA binding site (Ala<sup>88</sup>-Gly<sup>89</sup>-Pro<sup>90</sup>-Ile<sup>91</sup>) (Fig. 1, B and C), which is indicative of a slow local conformational equilibrium. The major conformer exhibits intense Gly<sup>89</sup>-H $\alpha$ -to-Pro<sup>90</sup>-H $\delta$  nuclear Overhauser effects (NOEs), reflecting a *trans*-Pro<sup>90</sup> peptide bond. In contrast, intense Gly<sup>89</sup>-H $\alpha$ -to-Pro<sup>90</sup>-H $\alpha$  NOEs diagnostic of a *cis*-Pro<sup>90</sup> peptidyl linkage were observed for the minor isomer (by the same criteria, Pro<sup>122</sup> contains a *cis* peptide bond, and all other proline peptide bonds are *trans*).

A total of 998 experimental distance restraints were used to generate an ensemble of 50 distance geometry structures with the use of the program DIANA (19). A stereoview of a best-fit superposition of the backbone atoms is shown in Fig. 2. The structure is composed of seven  $\alpha$  helices, two  $\beta$  hairpins, and an exposed partially ordered loop. Residues comprising these secondary structural elements are as follows: Pro<sup>1</sup> through Gln<sup>13</sup> form a  $\beta$  hairpin with a three-residue (Leu<sup>6</sup>-Gly<sup>8</sup>) turn; Ser<sup>16</sup> (the helix capping residue, N-cap) through Lys<sup>30</sup> form helix I; Ser<sup>33</sup> (N-cap) through Ala<sup>47</sup> form helix II, which is kinked at Pro<sup>38</sup> and changes from  $\alpha$ - to  $3^{10}$ -helicity at Ser<sup>44</sup>; Thr<sup>48</sup> (N-cap) through Thr<sup>58</sup> form helix III; Gln<sup>63</sup> through Leu<sup>83</sup> form helix IV; Pro<sup>85</sup> through Pro<sup>99</sup> form the CypA-binding loop, which contains a type II tight turn (Ala<sup>92</sup> through Gln<sup>95</sup>); Arg<sup>100</sup> through Ala<sup>105</sup>



**Fig. 2.** Stereoview of a best-fit superposition of the backbone C, C $\alpha$ , and N atoms of 50 HIV-1 CA<sub>151</sub> distance geometry models generated with DIANA (19). The NH<sub>2</sub>-terminal  $\beta$  hairpin and helices I through VII are colored orange, green, cyan, azure, purple, magenta, fuchsia, and red, respectively, and the disordered segments and loops are colored gray. Relevant structural statistics follow. Distance restraints: total, 998; intraresidue, 66; sequential, 201; medium-range, 308; long-range, 177; and hydrogen bond, 260 (four per hydrogen bond). Target function,  $0.51 \pm 0.05 \text{ \AA}^2$ ; maximum individual violation,  $\leq 0.17 \text{ \AA}$ ; number of distance violations per model greater than  $0.1 \text{ \AA}$ ,  $1.6 \pm 1.3$ ; maximum distance violation,  $0.12 \pm 0.02$ ; and sum of distance violations,  $4.0 \pm 0.4 \text{ \AA}$ . Pairwise rms deviations: backbone heavy atoms (C, C $\alpha$ , and N) of all helices (residues 17 through 30, 34 through 44, 49 through 57, 63 through 83, 111 through 118, and 127 through 144),  $0.74 \pm 0.15 \text{ \AA}$ ; backbone heavy atoms of helices plus  $\beta$  hairpins (residues 1 through 4, 10 through 13, 17 through 30, 34 through 44, 49 through 57, 63 through 83, and 111 through 144),  $0.85 \pm 0.16 \text{ \AA}$ ; all heavy atoms of residues 1 through 4, 10 through 13, 17 through 30, 34 through 44, 49 through 57, 63 through 83, and 111 through 144,  $1.51 \pm 0.14 \text{ \AA}$ .

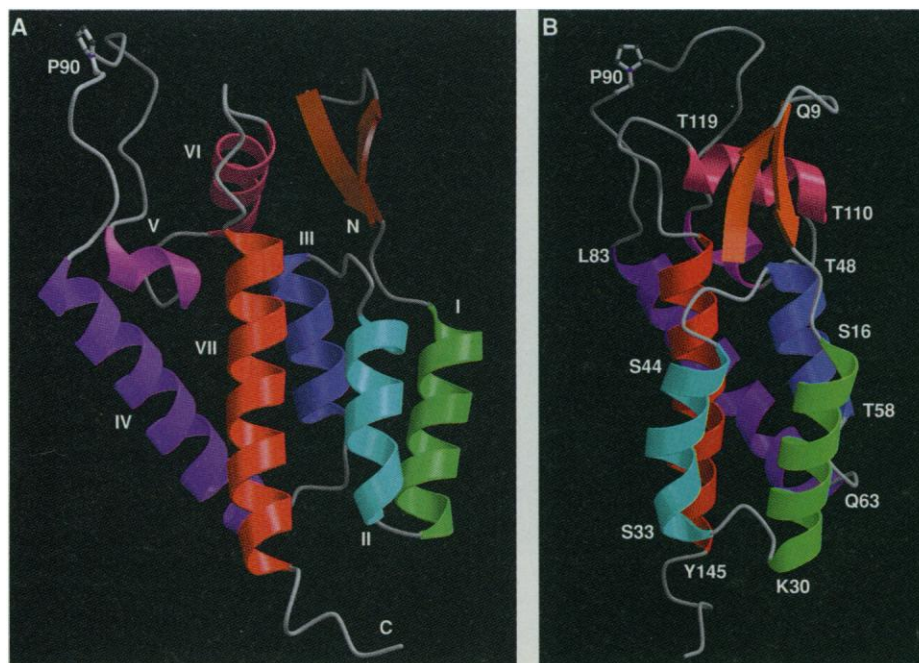


**Fig. 3.** Ribbon representations showing front (A) and edge-on (B) views of the arrowhead-shaped NH<sub>2</sub>-terminal core domain of HIV-1 CA. The domain is oriented with the tip of the arrowhead pointing toward the bottom of the figure. Heavy atoms of the *trans*-Pro<sup>90</sup> side chain in the exposed CypA-binding loop are included in the figure. Residues at the NH<sub>2</sub>- and COOH-termini of the helices,  $\beta$  hairpins, and CypA-binding loop are labeled (see Fig. 2 caption for coloring scheme).

form helix V; Gly<sup>106</sup> through Ser<sup>109</sup> form a turn; Thr<sup>110</sup> (N-cap) through Thr<sup>119</sup> form helix VI; His<sup>120</sup> through Pro<sup>125</sup> form a mini  $\beta$  hairpin structure; Val<sup>126</sup> through Tyr<sup>145</sup> form helix VII; and Ser<sup>146</sup> through Leu<sup>151</sup> form a short disordered stretch at the COOH-terminus. In general, residues within the disordered segments exhibit rapid backbone NH<sub>2</sub> exchange with water protons (20), and preliminary analysis of <sup>15</sup>N relaxation parameters indicates that these residues are indeed conformationally labile in solution.

The seven helices of CA<sub>151</sub> pack together through extensive hydrophobic interactions (Fig. 3), with the following interhelical interactions: helix I contacts helices II (antiparallel) and III (parallel); helix II contacts helices I (antiparallel), III (antiparallel), and VII (antiparallel); helix III contacts helices I (parallel), II (antiparallel), VI, and VII (parallel); helix IV contacts helix V (antiparallel) and makes a class II contact (tilted by 55°) with helix VII; helix V contacts helices IV (antiparallel) and VII; helix VI is nearly perpendicular to, and makes contacts with, helices III and VII; and helix VII contacts helices II, III, IV, V, and VI. The  $\beta$ -hairpin structures and the CypA-binding loop pack against helix VI and protrude from the domain in the same general direction (Fig. 3). The overall structure (21) resembles an arrowhead, with leading edge lengths of  $\sim$ 31

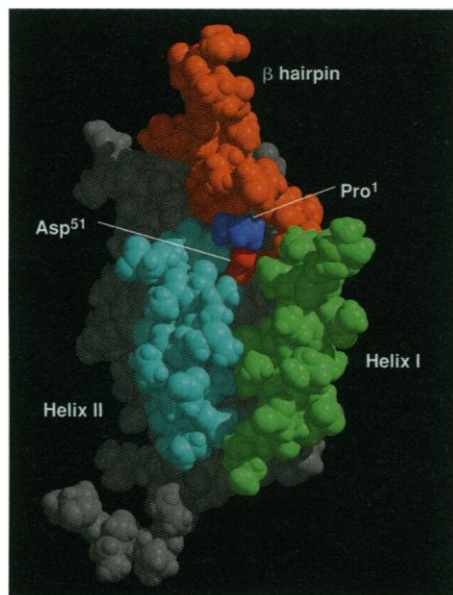


**Fig. 4.** Space-filling representation of HIV-1 CA<sub>151</sub>, showing the juxtaposition of the Pro<sup>1</sup>-NH<sub>2</sub><sup>+</sup> and Asp<sup>51</sup>-COO<sup>-</sup> charged groups. This salt bridge, which cannot exist in the Gag precursor protein, appears to stabilize the NH<sub>2</sub>-terminal  $\beta$  hairpin in the processed CA protein and may facilitate the structural reorganization that occurs during viral maturation. Coloring scheme: NH<sub>2</sub>-terminal  $\beta$  hairpin, orange; helix I, green; helix II, cyan; Pro<sup>1</sup>, blue; and Asp<sup>51</sup>, red.

$\text{\AA}$ , a trailing edge length of  $\sim$ 39  $\text{\AA}$ , and a thickness of  $\sim$ 16  $\text{\AA}$ . The HIV-1 CA<sub>151</sub> structure described here differs substantially from those of other RNA viral coat proteins (22) and from predicted HIV-1 CA structures used to interpret epitope mapping experiments and stimulate drug design (23).

In the immature virion, the CA<sub>151</sub> domain is NH<sub>2</sub>-terminally linked to the membrane-bound matrix protein (24) and COOH-terminally linked to the Gag assembly (CA-NC) and RNA binding (NC) domains. The capsid domain is thus likely to be oriented with the trailing edge of the arrowhead (and the CypA binding site) facing the viral membrane and the COOH-terminal tip pointing toward the center of the virus (that is, the viral membrane would reside on the top of Fig. 3A). Proteolytic maturation could then proceed by simple translocation of the CA and NC proteins toward the center of the virus without reordering or gross reorientation. This would place CypA between the matrix and capsid domains of the assembling Gag protein and subsequently on the outer surface of the mature viral capsid cone.

Although the rearrangements that accompany proteolytic maturation (1–3) are poorly understood at the molecular level, x-ray crystallographic studies of HIV-1 protease-peptide complexes reveal that protease binds the MA-CA junction in an extended conformation, with the first five residues of capsid protein projecting into a series of pockets in the enzyme (25). This mode of protease recognition is incompatible with the NH<sub>2</sub>-terminal  $\beta$ -hairpin structure of CA<sub>151</sub>, which suggests that the hairpin structure forms after proteolysis. In the cleaved capsid protein, the NH<sub>2</sub>-terminal NH<sub>2</sub><sup>+</sup> group of Pro<sup>1</sup> is oriented toward helix III and positioned to form a salt bridge with Asp<sup>51</sup> (Fig. 4). This aspartate is highly conserved (26), and is the only buried charged side chain in the protein (27). In the Gag precursor, Pro<sup>1</sup> would be uncharged and unable to form this salt bridge. Moreover, additional residues at the NH<sub>2</sub>-terminus of the  $\beta$ -hairpin structure would clash sterically with helices I, II, and III (Fig. 4). Thus, proteolytic processing probably triggers rearrangement of the NH<sub>2</sub>-terminal residues of CA from an extended conformation in the Gag polyprotein into the  $\beta$ -hairpin structure seen in the mature protein. This process is strikingly reminiscent of zymogen activation in the trypsin family of serine proteases, where proteolytic processing similarly allows rearrangement of the new NH<sub>2</sub>-terminus to form a salt bridge with a buried aspartate (28). We speculate that in the HIV-1 virus, formation of the  $\beta$  hairpin may alter CA-CA interactions and thereby serve as the trigger for formation of the capsid cone.

Several studies have established that the

loop connecting helices IV and V constitutes the primary CypA binding site. Mutations in this loop, including P90A, G89A, and  $\Delta$ 90-93 (15), abolish CypA binding in vitro and diminish CypA packaging and viral infectivity in culture (4, 5, 7, 8). Moreover, we have shown that transfer of the HIV-1 loop sequence <sup>87</sup>HAGPIA<sup>92</sup> confers CypA binding to chimeric capsid proteins containing otherwise nonbinding SIV sequences (29). In contrast, mutations involving the two prolines immediately outside the CypA binding site (P85A and P99A) lead to the production of noninfectious virions that nevertheless contain wild-type amounts of CypA (7). These prolines bracket the CypA binding loop and serve to break helices IV and V, respectively, and their substitution probably leads to protein misfolding. Pro<sup>93</sup> is located at the (i + 1) position of a type II turn within the CypA binding loop, and can be mutated to Ala without affecting CypA packaging, virion production, or infectivity (7). This represents a conservative substitution that would not be expected to destabilize the type II turn (30). It is interesting, however, that mutations on either side of this proline (A92E and G94D) result in viruses that retain their ability to package CypA but are resistant to cyclosporine (and nonimmunosuppressive analogs) and, indeed, depend on the drug for efficient replication (31). Although these substitutions are unlikely to affect the global structure of the HIV-1 CA core domain, the G94D substitution at the (i + 2) position is likely to have a major destabilizing effect on the type II turn (30). Both mutations may also affect the relative energies or kinetics of interconversion of the two CypA binding loop conformations.

The observation of two kinetically trapped conformations associated with the CypA binding site raises the possibility that the different loop conformations may facilitate distinct intermolecular interactions during virion morphogenesis. For example, Pro<sup>90</sup> could serve as a molecular switch for capsid assembly and disassembly, with CypA functioning either to flip the switch or to lock it in a particular state. Alternatively, the discrete flexible Pro<sup>90</sup> loop may simply provide a highly accessible handle for CypA binding. Agents that interfere with these or other essential capsid functions may now be designed with the use of structure-based approaches.

## REFERENCES AND NOTES

1. J. Wills and R. Craven, *AIDS* **5**, 639 (1991); H. Gelderblom *et al.*, *Membrane Interactions of HIV*, R. C. Aloia and C. C. Curtain, Eds. (Wiley-Liss, New York, 1992), pp 33–54; S. Modrow *et al.*, *Med. Microbiol. Immunol. Berlin* **184**, 177 (1994); E. Hunter, *Semin. Virol.* **5**, 71 (1994).
2. R. J. Mervis *et al.*, *J. Virol.* **62**, 3993 (1988); L. E. Henderson *et al.*, *ibid.* **66**, 1856 (1992).
3. H. G. Göttinger, J. G. Sodroski, W. A. Haseltine,

- Proc. Natl. Acad. Sci. U.S.A.* **86**, 5781 (1989); J. Jowett, D. Hockley, M. V. Nermut, I. M. Jones, *J. Gen. Virol.* **73**, 3079 (1992); A. von Pöhlitzki et al., *Virology* **193**, 981 (1993); S. S. Hong and P. Boulanger, *J. Virol.* **67**, 2787 (1993); C.-T. Wang and E. Barklis, *ibid.*, p. 4264; E. K. Franke, H. En Hui Yuan, K. L. Bossolt, S. P. Goff, J. Luban, *ibid.* **68**, 5300 (1994); N. Chazal, C. Carriere, B. Gay, P. Boulanger, *ibid.*, p. 111; P. Spearman, J. J. Wang, H. N. Vander, L. Ratner, *ibid.*, p. 3232.
4. T. Dorfman, A. Bukovsky, Å Öhagen, S. Höglund, H. G. Göttlinger, *J. Virol.* **68**, 8180 (1994).
5. A. S. Reicin et al., *ibid.* **69**, 642 (1995).
6. J. Luban, K. L. Bossolt, E. K. Franke, G. V. Kalpana, S. P. Goff, *Cell* **73**, 1067 (1993).
7. E. K. Franke, H. En Hui Yuan, J. Luban, *Nature* **372**, 359 (1994); D. Braaten, E. K. Franke, J. Luban, *J. Virol.* **70**, 3551 (1996).
8. M. Thali et al., *Nature* **372**, 363 (1994).
9. A. Billich et al., *J. Virol.* **69**, 2451 (1995); D. E. Ott et al., *AIDS Res. Hum. Retroviruses* **11**, 1003 (1995).
10. R. E. Handschumacher, M. W. Harding, J. Rice, R. J. Druggie, *Science* **226**, 544 (1984); G. Fischer, B. Wittmann-Liebhold, K. Lang, T. Kiefhaber, F. X. Schmid, *Nature* **337**, 476 (1989); Y. Thériault et al., *ibid.* **361**, 88 (1993); G. Pflügl et al., *ibid.*, p. 91.
11. A. Steinkasserer et al., *J. Virol.* **69**, 814 (1995).
12. L. S. Ehrlich, B. E. Agresta, C. A. Carter, *ibid.* **66**, 4874 (1992); S. Rosé et al., *Proteins Struct. Funct. Genet.* **13**, 112 (1992); I. Brooks, D. G. Watts, K. K. Soneson, P. Hensley, *Methods Enzymol.* **240**, 459 (1994).
13. A. J. Prongay et al., *Proc. Natl. Acad. Sci. U.S.A.* **87**, 9980 (1990).
14. Limited trypsin digestion of native and mutant (E159D) capsid proteins was performed as described previously [L. S. Ehrlich, B. E. Agresta, C. A. Gelfand, J. Jentoft, C. A. Carter, *Virology* **204**, 515 (1994)]. We selected the mutant capsid protein as an attractive candidate for proteolysis studies, because we hypothesized that the mutation, which abolishes Gag assembly in vivo (16), might also diminish capsid oligomerization or increase the accessibility of the assembly domain, or both. Conditions for 1D NMR-monitored proteolysis were as follows: 10 mg of protein and 5  $\mu$ g of trypsin in a 550- $\mu$ l volume of tris-HCl (100 mM) and dithiothreitol (DTT) (2 mM) at 25°C (pH 8.8). For CA<sub>E159D</sub>, spectral changes (and digestion) were complete in ~225 min, at which time the protease was inhibited with 40  $\mu$ g of soybean trypsin inhibitor.
15. Single-letter abbreviations for the amino acid residues are as follows: A, Ala; C, Cys; D, Asp; E, Glu; F, Phe; G, Gly; H, His; I, Ile; K, Lys; L, Leu; M, Met; N, Asn; P, Pro; Q, Gln; R, Arg; S, Ser; T, Thr; V, Val; W, Trp; and Y, Tyr.
16. F. Mammiano, Å. Öhagen, S. Höglund, H. G. Göttlinger, *J. Virol.* **68**, 4927 (1994).
17. DNA encoding the first 151 residues of HIV-1<sub>NL4-3</sub> capsid [A. Adachi et al., *ibid.* **59**, 284 (1986)] was amplified by polymerase chain reaction and subcloned into pET11a, and the resulting expression construct was transformed into BL21 (DE3) *E. coli* [F. W. Studier, A. H. Rosenberg, J. J. Dunn, J. W. Dubendorff, *Methods Enzymol.* **185**, 60 (1990)]. Soluble CA<sub>151</sub> protein was produced at ~30 mg liter<sup>-1</sup> after isopropyl- $\beta$ -D-thiogalactopyranoside induction and was purified to homogeneity by fractional ammonium sulfate precipitation and anion and cation exchange chromatographies. The purity and composition of the CA<sub>151</sub> protein were analyzed by SDS-PAGE and mass spectroscopy (MW<sub>calc</sub> = 16,701 daltons; MW<sub>obs</sub> = 16,700  $\pm$  4 daltons). A nonnative NH<sub>2</sub>-terminal methionine was quantitatively removed during expression; therefore, the NH<sub>2</sub>-terminus of the recombinant CA<sub>151</sub> protein is identical to the viral protein. Isotopically labeled CA<sub>151</sub> protein was prepared by growing the *E. coli* on minimal media containing either <sup>15</sup>NH<sub>4</sub>Cl or <sup>15</sup>NH<sub>4</sub>Cl-<sup>13</sup>C glucose. The amino acid sequence of CA<sub>151</sub> is P<sup>1</sup>-I-V-Q-N-L-Q-G-Q-M<sup>10</sup>-V-H-Q-A-I-S-P-R-T-L<sup>20</sup>-N-A-W-V-K-V-V-E-E-K<sup>30</sup>-A-F-S-P-E-V-I-P-M-F<sup>40</sup>-S-A-L-S-E-G-A-T-P-Q<sup>50</sup>-D-L-N-T-M-L-N-T-V-G<sup>60</sup>-G-H-Q-A-A-M-Q-M-L-K<sup>70</sup>-E-T-I-N-E-E-A-A-E-W<sup>80</sup>-D-R-L-H-P-V-H-A-G-P<sup>90</sup>-I-A-P-G-Q-M-R-E-P-R<sup>100</sup>-G-S-D-I-A-G-T-T-S-T<sup>110</sup>-L-Q-E-Q-I-G-W-M-T-H<sup>120</sup>-N-P-P-I-P-V-G-E-I-Y<sup>130</sup>-K-R-W-I-L-L-G-L-N-K<sup>140</sup>-I-V-R-M-Y-S-P-T-S-I<sup>150</sup>-L<sup>151</sup> (15).
18. NMR experiments were performed on unlabeled, <sup>15</sup>N-labeled, and <sup>13</sup>C-<sup>15</sup>N-labeled CA<sub>151</sub> protein samples with Bruker DMX and GE Omega PSG 600 MHz (<sup>1</sup>H) spectrometers equipped with Bruker triple resonance three-axis gradient probes. NMR samples were 1.3 mM CA<sub>151</sub> in D<sub>2</sub>O or 95%:5% H<sub>2</sub>O: D<sub>2</sub>O containing 25 mM NaH<sub>2</sub>PO<sub>4</sub> (pH 5.5) and 2 mM DTT. Higher CA<sub>151</sub> concentrations gave broader resonances, which suggests protein self-association. Raw NMR data were processed and analyzed with Felix (Biosym/Molecular Simulations, San Diego, CA) and NMRVIEW [B. A. Johnson and R. A. Blevins, *J. Biomol. NMR* **4**, 603 (1994)] software, respectively. 2D <sup>1</sup>H-<sup>15</sup>N HSQC and all 3D experiments involving samples in H<sub>2</sub>O were obtained with water-flip-back [S. Grzesiek and A. Bax, *J. Am. Chem. Soc.* **115**, 12593 (1993)] and field gradient pulses [M. Piotto, V. Saudek, V. Sklenar, *J. Biomol. NMR* **2**, 661 (1992)] to suppress the water signal without saturation. Sequential backbone assignments were made from 3D triple resonance experiments: HNCA, HNCOC, and HN(CO)CA [S. Grzesiek and A. Bax, *J. Magn. Reson.* **96**, 432 (1992)]; CB-CA(CO)NH [\_\_\_\_\_, *J. Am. Chem. Soc.* **114**, 6291 (1992)]; C(CO)NH [S. Grzesiek, J. Anglister, A. Bax, *J. Magn. Reson. B* **101**, 114 (1993)] with sensitivity-improved gradient coherence selection during the <sup>15</sup>N evolution period [D. R. Muhandiram and L. Kay, *ibid.* **103**, 203 (1994)]; and HCACO [L. E. Kay, M. Ikura, R. Tschudin, A. Bax, *J. Magn. Reson.* **89**, 496 (1990)]. Side chain carbon assignments were made from 3D HCCH-COSY [M. Ikura, L. E. Kay, A. Bax, *J. Biomol. NMR* **1**, 299 (1991)] and 3D HCCH-TOCSY data [23-ms mixing period; A. Bax, G. M. Clore, A. M. Gronenborn, *J. Magn. Reson.* **88**, 425 (1990)]. Side chain proton assignments were made from 3D <sup>15</sup>N-edited TOCSY data (32) obtained with a 70-ms clean-MLEV-17 mixing period [C. Griesinger, G. Otting, K. Wüthrich, R. R. Ernst, *J. Am. Chem. Soc.* **110**, 7870 (1988)] and sensitivity-improved gradient coherence selection [O. Zhang, L. E. Kay, J. P. Olivier, J. D. Forman-Kay, *J. Biomol. NMR* **4**, 845 (1994)]. NOE data (100-ms mixing period) were obtained from 2D NOESY data [J. Jeener, B. H. Meier, P. Bachmann, R. R. Ernst, *J. Chem. Phys.* **71**, 4546 (1979); S. Macura and R. R. Ernst, *Mol. Phys.* **41**, 95 (1980)]; 3D <sup>15</sup>N-edited NOESY-HSQC data (32); 3D <sup>15</sup>N-edited HMQC-NOESY-HSQC data [M. Ikura, A. Bax, G. M. Clore, A. M. Gronenborn, *J. Am. Chem. Soc.* **112**, 9020 (1990)]; 3D <sup>13</sup>C-edited HMQC-NOESY data [S. W. Fesik and E. R. P. Zuiderweg, *J. Magn. Reson.* **78**, 588 (1988)]; 4D <sup>13</sup>C, <sup>13</sup>C-edited HMQC-NOESY-HMQC data [G. Vuister et al., *J. Magn. Reson. B* **101**, 210 (1993)]; and 4D <sup>13</sup>C, <sup>15</sup>N-edited HMQC-NOESY-HSQC data [L. E. Kay, G. M. Clore, A. Bax, A. M. Gronenborn, *Science* **249**, 411 (1990); D. R. Muhandiram, G. Y. Xu, L. E. Kay, *J. Biomol. NMR* **3**, 463 (1993)].
19. P. Güntert, W. Braun, K. Wüthrich, *J. Mol. Biol.* **217**, 517 (1991); P. Güntert and K. Wüthrich, *J. Biomol. NMR* **1**, 447 (1991). Secondary structural elements were identified by analysis of NOE cross-peak patterns [K. Wüthrich, *NMR of Proteins and Nucleic Acids*. (Wiley, New York, 1986)] and <sup>13</sup>C $\alpha$ , <sup>13</sup>CO, and <sup>1</sup>H $\alpha$  chemical shift indices [S. Spera and A. Bax, *J. Am. Chem. Soc.* **113**, 5490 (1991); D. S. Wishart, B. D. Sykes, F. M. Richards, *J. Mol. Biol.* **222**, 311 (1991); *Biochemistry* **31**, 1647 (1992); D. S. Wishart and B. D. Sykes, *J. Biomol. NMR* **4**, 171 (1994)]. Only functional restraints were included in the calculations (for example, in cases where a proton exhibited NOEs of different intensities to geminal methylene protons, restraints were only employed for the stronger of the two cross peaks). Initial structure calculations were performed without hydrogen-bond restraints, affording structures with penalties in the range 0.3 to 1.0 Å<sup>2</sup> and best-fit backbone root mean square (rms) deviations of 1.3  $\pm$  0.3 Å. Backbone hydrogen bond restraints identified with the use of DIANA, and additional NOE restraints, were included in subsequent rounds of refinement, which led to improved convergence but did not alter the global fold. Color figures were generated with the Midas-plus
- [T. E. Ferrin, C. C. Huang, L. E. Jarvis, R. Langridge, *J. Mol. Graph.* **6**, 13 (1988); Molscript [P. J. Kraulis, *J. Appl. Crystallogr.* **24**, 946 (1991)], and Raster-3D [D. J. Bacon and W. F. Anderson, *J. Mol. Graph.* **6**, 219 (1988); E. A. Merritt and M. E. P. Murphy, *Acta Crystallogr.* **D50**, 869 (1994)] software packages.
20. Backbone NH protons that undergo rapid exchange with water protons were identified from MEXICO NMR data [G. Gemmecker, W. Jahnke, H. Kessler, *J. Am. Chem. Soc.* **115**, 11620 (1993); S. Koide, W. Jahnke, P. E. Wright, *J. Biomol. NMR* **6**, 306 (1995)] collected with exchange intervals of 25, 50, 75, and 100 ms.
21. A search of the Brookhaven Protein Data Bank for homologous structures with the DALI program [L. Holm and C. Sander, *J. Mol. Biol.* **233**, 123 (1993)] revealed homotetrameric cyanomet hemoglobin from the inkeeper worm *Urechis caupo* [P. R. Kolatkar et al., *Acta Crystallogr.* **B48**, 191 (1992)] as the only potential homolog (best-fit rms deviations = 6.5 Å, z = 2.0).
22. For examples, see the following: M. Rossmann and J. Johnson, *Annu. Rev. Biochem.* **58**, 533 (1989); M. G. Rossmann et al., *Nature* **317**, 145 (1985); J. M. Hogle et al., *Science* **229**, 1358 (1985); S. C. Harrison et al., *Nature* **276**, 368 (1978); C. Abad-Zapatero et al., *ibid.* **286**, 33 (1980); L. Liljas et al., *J. Mol. Biol.* **159**, 93 (1982); K. Valegard et al., *Nature* **345**, 36 (1990); J. Grimes et al., *ibid.* **373**, 167 (1995); A. K. Basak et al., *J. Virol.* **70**, 3797 (1996).
23. A. R. M. Coates, J. Cookson, G. J. Barton, M. J. Zvelebil, M. J. E. Sternberg, *Nature* **326**, 549 (1987); M. G. Rossmann, *Proc. Natl. Acad. Sci. U.S.A.* **85**, 4625 (1988); P. Argos, *EMBO J.* **8**, 779 (1989); J. P. M. Langedijk, J. J. Schalken, M. Tersmette, J. G. Huisman, R. H. Meloen, *J. Gen. Virol.* **71**, 2609 (1990); V. Robert-Hebmann et al., *Mol. Immunol.* **29**, 729 (1992).
24. S. Mathews et al., *Nature* **370**, 666 (1994); M. Masiah et al., *J. Mol. Biol.* **244**, 198 (1994); Z. Rao et al., *Nature* **378**, 743 (1995); C. P. Hill, D. Worthylake, D. P. Bancroft, A. M. Christensen, W. I. Sundquist *Proc. Natl. Acad. Sci. U.S.A.* **93**, 3099 (1996).
25. A. Wlodawer and J. W. Erickson, *Annu. Rev. Biochem.* **62**, 543 (1993).
26. R. Meyers, B. Korber, S. Wain-Hobson, R. F. Smith, G. N. Pavlakis, Eds. *Human Retroviruses and AIDS* (Los Alamos National Laboratory, Los Alamos, NM, 1995).
27. <sup>1</sup>H resonances were not observed for the labile NH<sub>2</sub>-terminal amine, but the orientation of Pro<sup>1</sup> was established unambiguously by observed NOEs between the following atom pairs: Pro<sup>1</sup>-H $\alpha$  to Ala<sup>47</sup>-H $\alpha$ , Ile<sup>2</sup>-HN to Pro<sup>1</sup>-H $\alpha$ , Ile<sup>2</sup>-HN to Gly<sup>46</sup>-H $\alpha$ , and Ile<sup>2</sup>-HN to Ala<sup>47</sup>-H $\alpha$ .
28. P. B. Sigler, D. M. Blow, B. W. Mathews, R. Henderson, *J. Mol. Biol.* **35**, 143 (1968); J. McConn, G. D. Fasman, G. P. Hess, *ibid.* **39**, 551 (1969); S. T. Freer et al., *Biochemistry* **9**, 1997 (1970); A. R. Fersht, *J. Mol. Biol.* **64**, 497 (1972); J. Birktoft et al., *Biochemistry* **15**, 4481 (1976); A. A. Kossiakoff et al., *ibid.* **16**, 654 (1977); H. Felhammer et al., *J. Mol. Biol.* **111**, 415 (1977); H. Huber and W. Bode, *Acc. Chem. Res.* **11**, 114 (1978); L. Hedstrom et al., *Biochemistry* **35**, 4515 (1996).
29. S. Yoo, D. Myszkla, C.-Y. Yeh, M. McMurray, W. I. Sundquist, in preparation.
30. C. M. Wilmot and J. M. Thornton, *J. Mol. Biol.* **203**, 221 (1988).
31. C. Aberham, S. Weber, W. Phares, *J. Virol.* **70**, 3536 (1996); D. Braaten et al., *J. Virol.*, in press.
32. D. Marion et al., *Biochemistry* **28**, 6150 (1989).
33. R. K. Gitti et al., data not shown.
34. Supported by NIH grant AI30917 (M.F.S.), an award from the Searle Scholars Program (W.I.S.), a grant from the Lucille P. Markey Charitable Trust, and the University of Utah Cancer Center Support Grant (CA 42014). NMR instrumentation was purchased with partial support from NIH grant GM 42561. J.W. is supported by a Meyerhoff scholarship from the University of Maryland Baltimore County (UMBC). We are grateful to T. O'Hern (Howard Hughes Medical Institute, UMBC) and M. Zawrotny (UMBC) for technical support.

31 May 1996; accepted 18 June 1996